TR - H - 151

Bifurcations in Traveling Salesman Problem

Shin ISHII *Masaaki SATO*

1995. 6. 6

ATR人間情報通信研究所

〒619-02 京都府相楽郡精華町光台2-2 ☎ 0774-95-1011

ATR Human Information Processing Research Laboratories
2-2, Hikaridai, Seika-cho, Soraku-gun, Kyoto 619-02 Japan
Telephone: +81-774-95-1011
Facsimile: +81-774-95-1008

Bifurcations in traveling salesman problem

Shin Ishii **Masaaki Sato**

ATR Human Information Processing Research Laboratories
2-2 Hikaridai, Seika-cho, Soraku-gun, Kyoto 619-02 JAPAN

Abstract

In the analog Hopfield network and the mean field theory (MFT) of the Boltzmann machine, bifurcations of solutions occur during the course of the annealing procedure. In this report, we investigate the MFT bifurcation processes when MFT is applied to traveling salesman problems (TSPs). A TSP has two types of symmetries, i.e., cyclic and reverse. These symmetries affect the bifurcation structure. This report also describes some features of the MFT annealing procedure. The algorithm does not necessarily give unique solutions, and it does not guarantee the optimal solution. Consequently, MFT annealing has a non-deterministic property and results in "not-so-bad" solutions, in general. To overcome the limitations, we also propose a couple of modified algorithms.

1 Introduction

The analog Hopfield network always converges to a local minimum of its Lyapunov function.[1] When the slope of the sigmoidal output function becomes large, the Lyapunov function is nearly equal to the energy function, which has a quadratic form of the state variables. By utilizing this feature, the Hopfield network can be used for solving combinatorial optimization problems defined as a minimization of the quadratic energy function.[2]

Peterson and Anderson[3] showed that the Hopfield network is equivalent to the mean field theory (MFT) of the Boltzmann machine. The Lyapunov function of the Hopfield network corresponds to the free energy function in the MFT. This implies that the Hopfield network finds a local minimum of the free energy function in the MFT.

Wilson and Pawley[7] reported that the Hopfield network is not a good algorithm for solving combinatorial optimization problems when the problem scale is not very small. Neural network approaches need some additional mechanisms for relatively large scale problems. One of them is a gradual slope enlarging of the sigmoidal output function, i.e., a gradual lowering of the system's "temperature," which corresponds to a well-known annealing mechanism. This is the mean field annealing (MFA) algorithm.[4, 6] The free energy function has a unique minimum at high temperature. On the other hand, it has a lot of minima at low temperature, which correspond to local minima of the quadratic energy function. Then, as the temperature is gradually lowered, bifurcations occur and new minima are generated.

In this report, we investigate bifurcation processes of the MFT solutions when MFT is applied to traveling salesman problems (TSPs). A TSP has two types of symmetries, i.e., cyclic and reverse. These symmetries affect the bifurcation structure. This report also describes some features of the MFA procedure. The algorithm does not necessarily give unique solutions, and it does not guarantee the optimal solution. Consequently, MFT annealing has a non-deterministic property and results in "not-so-bad" solutions, in general. To overcome the limitations, we also propose a couple of modified algorithms.

2 Mean field theory

Many $\mathcal{NP}$-complete optimization problems can be described as a quadratic energy minimization problem for binary variables $S_n (= 0 \text{ or } 1)$:

$$E(\mathbf{S}) = \frac{1}{2} \sum_{n,m=1}^{N} W_{nm} S_n S_m + \sum_{n=1}^{N} J_n S_n, \tag{2.1}$$

where $W_{nm} = W_{mn}$. In this formulation, constraints are treated as soft constraints. The values of the parameters W_{nm} and J_n are determined for each problem. In the MFT, analog variable $V_n \in [0, 1]$, which represents the probability that the binary

variable S_n takes the value 1, is introduced. Then, the free energy is given as follows:

$$F(\mathbf{V}) = E(\mathbf{V}) + T \cdot \sum_n [V_n \log V_n + (1 - V_n) \log(1 - V_n) + \log 2], \tag{2.2}$$

where T corresponds to the temperature in statistical mechanics. A minimum of the MFT free energy, which corresponds to an equilibrium point in statistical mechanics with the energy (2.1), satisfies the stationary condition of the free energy function:

$$U_n = -\sum_m W_{nm} V_m - J_n, \tag{2.3a}$$

$$V_n = G(U_n) \equiv \frac{1}{1 + e^{-U_n/T}}. \tag{2.3b}$$

The solution of this MFT equation can be obtained by using the analog Hopfield network[1]:

$$\tau \frac{dU_n(t)}{dt} = -\frac{\partial F}{\partial V_n} = -U_n(t) - \sum W_{nm} V_m(t) - J_n, \tag{2.4a}$$

$$V_n(t) = G(U_n(t)), \tag{2.4b}$$

or the asynchronous MFT equation.

At high temperature ($T \to \infty$), the free energy (2.2) is dominated by the entropy term, i.e., the second term of the r.h.s. of (2.2), and there is a unique minimum. At low temperature ($T \to 0$), the free energy function $F(\mathbf{V})$ is nearly equal to the energy function $E(\mathbf{V})$. In addition, local minima of the energy function occur at the hypercube corners ($V_n \in \{0, 1\}$) if $W_{nn} = 0$. Therefore, at low temperature, there are local minima of the free energy function (2.2) that correspond to those of the original energy function (2.1). If the temperature is fixed at a low value, which local minimum is found is dependent on the initial condition.

In order to get a good local minimum of the energy function (2.1), mean field annealing (MFA) can be used. First, the MFT equation (2.3) is solved at high temperature, and a unique minimum is obtained. Then, after the temperature is slightly lowered, the MFT equation is solved starting from the higher temperature solution. By continuing this process, one can get a low temperature solution that corresponds to a local minimum of the energy function (2.1). During the course of temperature lowering, bifurcations occurs and new minima are generated. These bifurcation processes are dependent on the structurally stable symmetries in the problem.

3 Symmetries in TSP

Let us consider the case of TSPs. An energy function for a TSP is given by

$$E(\mathbf{V}) = \frac{1}{2} \sum_{a,b,n,m=1}^{N} W_{a,n;b,m} V_{a,n} V_{b,m} + \sum_{a,n=1}^{N} J_{a,n} V_{a,n} + E_0$$

$$= \frac{1}{2}\sum_{a,b,n=1}^{N} D_{ab}V_{a,n}(V_{b,(n+1)} + V_{b,(n-1)}) \tag{3.1}$$

$$+ \frac{A}{2}\left[\sum_a(\sum_n V_{a,n} - 1)^2 + \sum_n(\sum_a V_{a,n} - 1)^2 + 2\sum_{a,n} V_{a,n}(1 - V_{a,n})\right],$$

where N is the number of cities, $V_{a,n}$ represents the probability that the salesman visits city a at the n-th visit, and D_{ab} denotes the distance between city a and city b. The free energy function is defined as:

$$F(\mathbf{V}) = E(\mathbf{V}) + T \cdot \sum_{a,n}[V_{a,n}\log V_{a,n} + (1 - V_{a,n})\log(1 - V_{a,n}) + \log 2]. \tag{3.2}$$

The energy and free energy functions are invariant under the N-th order cyclic transformation: $\mathbf{V} \longrightarrow \mathcal{T}_m^{[N]}\mathbf{V}$ $(m = 1, ..., N-1)$, where $(\mathcal{T}_m^{[N]}\mathbf{V})_{a,n} = V_{a,n+m}$, and the N-th order reverse transformation: $\mathbf{V} \longrightarrow \mathcal{R}_m^{[N]}\mathbf{V}$ $(m = 0, 1, ...N-1)$, where $(\mathcal{R}_m^{[N]}\mathbf{V})_{a,n} = V_{a,m-n}$. Due to these symmetries, a solution of an N-city TSP has $2N$ equivalent representations.

There is a symmetric stationary solution $\mathbf{V}^s$ of the free energy function for any T: $V^s_{a,n} = V^s_a$ $(a, n = 1, ..., N)$. $\mathbf{V}^s$ is a stationary solution of the reduced free energy function:

$$F_s/N = \sum_{a,b} D_{ab}V_aV_b + \frac{A}{2}[N\sum_a(V_a - 1/N)^2 + (\sum_a V_a - 1)^2 + 2\sum_a V_a(1 - V_a)]$$

$$+T\sum_a[V_a\log V_a + (1 - V_a)\log(1 - V_a)]. \tag{3.3}$$

Since $\mathcal{T}_m^{[N]}\mathbf{V}^s$ coincides with $\mathbf{V}^s$, $\mathbf{V}^s$ has the N-th order cyclic symmetry. Moreover, since $\mathcal{R}_m^{[N]}\mathbf{V}^s$ coincides with $\mathbf{V}^s$, $\mathbf{V}^s$ has the N-th order reverse symmetry. Since the free energy function (3.2) has a unique minimum at high temperature, the unique minimum must be $\mathbf{V}^s$. Below the critical temperature, this symmetry breaks down and partially symmetric solutions or non-symmetric solutions appear.

In what follows, we consider a bifurcation process that occurs at $\mathbf{V} = \mathbf{V}^*$ and $T = T_c$. Let us assume that $\mathbf{V}^*$ has the N-th order cyclic symmetry. Although N is the number of cities, the following discussion can be expanded to the case where N is a divisor of the number of cities. The bifurcation point satisfies the stationary condition: $\partial F/\partial V_{a,n}|_{V^*,T_c} = 0$. Near the bifurcation point, the free energy (3.2) can be expressed as a Taylor series with respect to $\delta V_{a,n} = V_{a,n} - V^*_{a,n}$, and $\epsilon = T - T_c$:

$$F(\mathbf{V}^* + \delta\mathbf{V}, T_c + \epsilon) = F(\mathbf{V}^*, T_c) + \frac{1}{2}\sum_{a,b,n,m} M_{a,n;b,m}\delta V_{a,n}\delta V_{b,m}$$

$$+\frac{1}{3!}\sum_{a,n} a[1]_{a,n}\delta V^3_{a,n} + \frac{1}{4!}\sum_{a,n} a[2]_{a,n}\delta V^4_{a,n} + ... \tag{3.4}$$

$$+\epsilon\sum_{a,n} b[1]_{a,n}\delta V_{a,n} + \frac{1}{2}\epsilon\sum_{a,n} b[2]_{a,n}\delta V^2_{a,n} + ...,$$

where $M_{a,n;b,m} = W_{a,n;b,m} + \delta_{a,b}\delta_{n,m}T_c/(V^*_{a,n}(1 - V^*_{a,n}))$, $a[1]_{a,n} = T_c(2V^*_{a,n} - 1)/(V^*_{a,n}(1 - V^*_{a,n}))^2$, $a[2]_{a,n} = 2T_c(3(V^*_{a,n})^2 - 3V^*_{a,n} + 1)/(V^*_{a,n}(1 - V^*_{a,n}))^3$, $b[1]_{a,n} = \log(V^*_{a,n}/(1 - V^*_{a,n}))$, and $b[2]_{a,n} = 1/(V^*_{a,n}(1 - V^*_{a,n}))$.

Because of the invariance under the N-th order cyclic transformation, the curvature matrix of the free energy function, $\mathbf{M}$, has the symmetry:

$$M_{a,n;b,m} = M_{a,(n+k);b,(m+k)} = M_{a,N;b,(m-n)} \qquad (k = 1, ..., N).$$

Then, $\mathbf{M}$ is commutative with $\mathcal{T}_m^{[N]}$; eigenvectors of the curvature matrix $\mathbf{M}$ are also eigenvectors of the N-th order cyclic transformation $\mathcal{T}_m^{[N]}$. The eigenmodes of $\mathbf{M}$ are characterized by the N-th roots of 1:

$$\alpha(k) = \exp(2\pi ki/N), \quad \alpha(k)^N = 1, \quad \bar{\alpha}(k) = \alpha(k)^{-1} = \alpha(-k), \quad k \in \Gamma_N, \tag{3.5}$$

where $\Gamma_N = \{0, \pm 1, ..., \pm(N/2-1), N/2\}$ for even N, and $\Gamma_N = \{0, \pm 1, ..., \pm(N-1)/2\}$ for odd N. The eigenvector of $\mathbf{M}$ associated with $\alpha(k)$ can be written as: $v_a(k) \cdot \alpha(k)^n$ $(a, n = 1, ..., N)$. Then, the reduced eigen equation for $v_a(k)$ is written as

$$\sum_{b=1}^{N} \Omega(k)_{a,b} v_b(k) = \lambda v_a(k) \qquad (a = 1, ..., N), \tag{3.6}$$

where $\Omega(k)_{a,b} = \sum_{n=1}^{N} M_{a,N;b,n}\alpha(k)^n$. By using the fact that $\mathbf{M}$ is a real symmetric matrix, it can be proved that $\mathbf{\Omega}(k)$ is also a real symmetric matrix and $\mathbf{\Omega}(k) = \mathbf{\Omega}(-k)$ holds. This implies that $v_a(-k) = v_a(k)$ and eigenvectors of $\mathbf{M}$, $(v_a(k)\alpha(k)^n)$ and $(v_a(k)\alpha(-k)^n)$, have the same real eigenvalue, so that an eigenvalue corresponding to complex $\alpha(k)$ is doubly degenerate and an eigenvalue corresponding to real $\alpha(k)(= 1 \text{ or } -1)$ is simple. Let $v_a(r,k)$ and $\lambda(r,k)$ be the r-th $(r = 0, 1, ..., N-1)$ eigenvector and the corresponding eigenvalue of (3.6), respectively. Then, $\delta V_{a,n}$ can be expressed using the eigenmode coordinate $z_{r,k}$ as:

$$\delta V_{a,n} = \sum_{k \in \Gamma_N} \sum_{r=0}^{N-1} z_{r,k} \cdot (v_a(r,k) \cdot \alpha(k)^n) \qquad (a, n = 1, ..., N). \tag{3.7}$$

Since $\delta V_{a,n}$ is real and $v_a(r,k) = \bar{v}_a(r,k) = v_a(r,-k)$, $\bar{z}_{r,k} = z_{r,-k}$ holds. In terms of the eigenmode coordinate $z_{r,k}$, the N-th order cyclic transformation becomes

$$z_{r,k} \longrightarrow \mathcal{T}_m^{[N]} z_{r,k} = \alpha(k)^m z_{r,k} \qquad (m = 1, ..., N-1). \tag{3.8}$$

When the solution $\mathbf{V}^*$ has the N-th order reverse symmetry, the N-th order reverse transformation for the eigenmode coordinate $z_{r,k}$ becomes

$$z_{r,k} \longrightarrow \mathcal{R}_m^{[N]} z_{r,k} = \chi(r,k)\alpha(k)^m \bar{z}_{r,k} \qquad (m = 0, 1, ..., N-1). \tag{3.9}$$

The value of $\chi(r,k)$ is $+1$ or -1, and it is called the reverse symmetry index.

4 Bifurcations in TSP

4.1 Symmetry breaking bifurcation

First, we consider a case where $\mathbf{V}^*$ has the 5th order cyclic and reverse symmetries, a complex $\alpha(1)$ becomes a zero eigenvalue mode, and $\chi(r,1) = 1$. The indices a and

r are neglected for convenience. The free energy function (3.4) is described in terms of eigen coordinate $\{z_k | k = 0, \pm 1, \pm 2\}$ as:

$$
\begin{aligned}
&F(\mathbf{V}^* + \delta\mathbf{V}, T_c + \epsilon)/5 = \\
&\quad \frac{1}{2}\lambda(0) z_0^2 + \lambda(2)\bar{z}_2 z_2 + \epsilon b[1] z_0 + \frac{1}{2}\epsilon b[2](z_0^2 + 2(\bar{z}_1 z_1 + \bar{z}_2 z_2)) \\
&\quad + \frac{1}{3!}a[1](z_0^3 + 6z_0(\bar{z}_1 z_1 + \bar{z}_2 z_2) + 3(z_1^2 \bar{z}_2 + \bar{z}_1^2 z_2 + z_1 z_2^2 + \bar{z}_1 \bar{z}_2^2)) \qquad (4.1) \\
&\quad + \frac{1}{4!}a[2]\{z_0^4 + 12 z_0^2(\bar{z}_1 z_1 + \bar{z}_2 z_2) + 12 z_0(\bar{z}_2 z_1^2 + z_2 \bar{z}_1^2 + z_1 z_2^2 + \bar{z}_1 \bar{z}_2^2) \\
&\qquad + 6((\bar{z}_1 z_1)^2 + (\bar{z}_2 z_2)^2 + 4(\bar{z}_1 z_1)(\bar{z}_2 z_2)) + 4(z_1^3 z_2 + \bar{z}_1^3 \bar{z}_2 + z_1 \bar{z}_2^3 + \bar{z}_1 z_2^3)\} + \ldots \ ,
\end{aligned}
$$

where $a[1]_n = a[1]$ $(n = 1, ..., 5)$, and so on. Only the invariant combinations under the 5th order cyclic and reverse transformations appear in (4.1). By considering the leading order terms in (4.1), the non-zero eigenvalue modes z_0 and z_2 are of order ϵ, and the zero eigenvalue mode z_1 is of order $\epsilon^{1/2}$ at the stationary point. By assuming that z_1 is of order $\epsilon^{1/2}$, the stationary conditions for z_0 and z_2 can be solved successively, and z_0 and z_2 can be expressed in terms of z_1:

$$z_0 = C_{0,1}^{(2)}\epsilon + C_{0,2}^{(2)}(\bar{z}_1 z_1) + C_{0,1}^{(4)}\epsilon(\bar{z}_1 z_1) + C_{0,2}^{(4)}(\bar{z}_1 z_1)^2 + C_{0,1}^{(5)}(z_1^5 + \bar{z}_1^5) + \ldots \quad (4.2a)$$

$$z_2 = C_{2,1}^{(2)} z_1^2 + C_{2,1}^{(3)} \bar{z}_1^3 + \epsilon C_{2,1}^{(4)} z_1^2 + C_{2,2}^{(4)} z_1^2(\bar{z}_1 z_1) + \ldots, \quad (4.2b)$$

where $C^{(s)}$'s are coefficients of order $\epsilon^{s/2}$ which can be determined by considering the terms of order $\epsilon^{s/2}$ in $\partial F/\partial z_k = 0$. Substituting (4.2) into (4.1), one can get the effective free energy for the zero eigenvalue mode z_1:

$$F(z_1) = \frac{1}{2}d_1\epsilon(\bar{z}_1 z_1) + \frac{1}{4}d_2(\bar{z}_1 z_1)^2 + \frac{1}{5}d_3(z_1^5 + \bar{z}_1^5) + \ldots, \quad (4.3)$$

where $d_1/5 = 2b[2] - 2a[1]b[1]/\lambda(0), d_2/5 = a[2] - 2a[1]^2/\lambda(0) - a[1]^2/\lambda(2)$, and $d_3/5 = 5a[1]^3/(8\lambda(2)^2) - 5a[1]a[2]/(12\lambda(2)) + a[3]/24$. This effective free energy function is composed with the elementary invariant combinations, $(\bar{z}_1 z_1)$ and $(z_1^5 + \bar{z}_1^5)$, because of the invariance under the 5th order cyclic and reverse transformations. The leading order terms, $\epsilon(\bar{z}_1 z_1)$ and $(\bar{z}_1 z_1)^2$ in (4.3), are invariant under the continuous transformation: $z_1 \longrightarrow e^{i\theta} z_1$ $(0 \leq \theta < 2\pi)$; the leading order solution is continuously degenerate. However, the higher order term, $(z_1^5 + \bar{z}_1^5)$, which is not invariant under the continuous transformation, breaks this degeneracy. Defining a polar coordinate by $z_1 = \gamma e^{i\phi}$ the free energy (4.3) can be written as

$$F(\gamma, \phi) = \frac{1}{2}d_1\epsilon\gamma^2 + \frac{1}{4}d_2\gamma^4 + \frac{2}{5}d_3\gamma^5 \cos 5\phi + \ldots \quad (4.4)$$

The stationary conditions: $\partial F/\partial\gamma = 0$ and $\partial F/\partial\phi = 0$, have a symmetric solution:

$$\gamma = 0 \quad (4.5)$$

for any ϵ. If $(\epsilon d_1/d_2) < 0$, there is another set of solutions:

$$\gamma = \sqrt{(-d_1/d_2)\epsilon} + O(\epsilon) \tag{4.6a}$$

$$\phi = j\pi/5 \qquad (j = 0, 1, ..., 9)\,. \tag{4.6b}$$

In addition, by considering the curvature matrix of (4.4), the stability of the solutions (4.5) and (4.6) can be determined. If $d_1\epsilon > 0$, (4.5) is stable and all of (4.6) are unstable. If $d_1\epsilon < 0$, (4.5) and half of (4.6) are unstable, and the other half of (4.6) are stable. In the latter case, if $d_3 < 0\ (> 0)$, j:even (odd) solutions of (4.6) are stable. Let us denote j:even (odd) solutions by

$$z_1^e[J] = \gamma e^{i2\pi J/5} \tag{4.7a}$$

$$z_1^o[J] = \gamma e^{(i2\pi J/5)+(i\pi/5)} \qquad (J = 0, 1, ..., 4). \tag{4.7b}$$

Under the 5th order cyclic and reverse transformations, a j:even (odd) solution is transformed to another j:even (odd) solution. Moreover, it is proved that they have a 1st order reverse symmetry:

$$\mathcal{R}^{[5]}_{m[J]} z_1^e[J] = z_1^e[J] \quad \text{for } m[J] = 2J \pmod 5, \tag{4.8a}$$

$$\mathcal{R}^{[5]}_{m'[J]} z_1^o[J] = z_1^o[J] \quad \text{for } m'[J] = 2J + 1 \pmod 5. \tag{4.8b}$$

Therefore, the cyclic symmetry is broken while the reverse symmetry is preserved; this is a cyclic symmetry breaking bifurcation.

Four types of cyclic symmetry breaking bifurcation diagrams are illustrated in Figure 1. In Fig. 1a, where $d_1 > 0, d_2 > 0$, a minimum with the 5th order cyclic symmetry for $T > T_c$ becomes a saddle point and five minima appear together with five saddle points for $T < T_c$. In Fig. 1d, where $d_1 > 0, d_2 < 0$, a minimum with the 5th order cyclic symmetry for $T > T_c$ becomes a saddle point, and there are ten saddle points without the cyclic symmetry for $T > T_c$. Fig. 1b is the case: $d_1 < 0, d_2 > 0$, and Fig. 1c is the case: $d_1 < 0, d_2 < 0$. All of the solutions have the reverse symmetry.

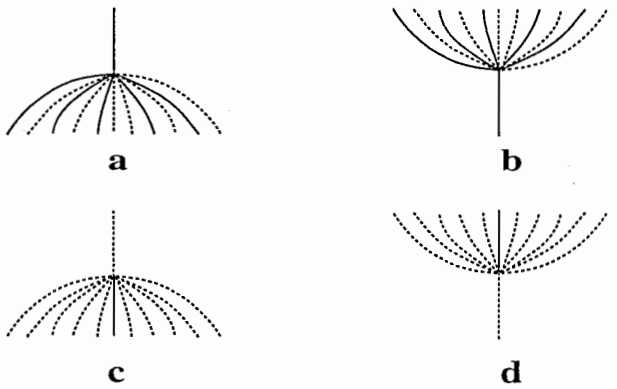

Figure 1

4.2 Possible bifurcations

Here, we describe all of the possible bifurcations in the MFA procedure for a TSP. They are classified by the symmetry of the eigenvector that corresponds to the zero eigenvalue mode of the free energy curvature matrix at the bifurcation point.

- $N = 1$ case
  If $\mathbf{V}^*$ has no symmetry, i.e., $N = 1$, a saddle-node bifurcation occurs. $2N$ equivalent minima appear or disappear simultaneously. This type of bifurcations are most typically observed.

- $\alpha(0)$ case
  When $\mathbf{V}^*$ has the N-th order cyclic symmetry and no reverse symmetry, and one of the eigenvectors that correspond to $\alpha(0)(= 1)$ becomes a zero eigenvalue mode, a saddle-node bifurcation occurs. If $\mathbf{V}^*$ also has the reverse symmetry and the corresponding χ is 1, the reverse symmetry is preserved. If the corresponding χ is -1, a pitchfork bifurcation (or, a reverse symmetry breaking bifurcation) occurs.

- $\alpha(N/2)$ case
  When N is even and one of the eigenvectors that correspond to $\alpha(N/2)(= -1)$ becomes a zero eigenvalue mode, a pitchfork bifurcation occurs.

- $\alpha(K)$ case (cyclic symmetry breaking)
  Almost the same argument as in Sec. 4.1 can be given for general N and K $(\neq 0, N/2)$ if there is no common divisor for K and N. In this case, the bifurcation diagrams are the same as in Fig. 1 except that five equivalent solutions are replaced by N equivalent solutions. If $\mathbf{V}^*$ also has the reverse symmetry, it is preserved, in general. However, there is an exception, that is, when N is odd and the reverse symmetry index χ is -1. In this case, the relation like in (4.8) does not hold, and the reverse symmetry is broken. As a result, the N solutions in the bifurcation diagrams are replaced by $2N$ solutions with no symmetry.

- partial cyclic symmetry breaking
  Let us assume that the greatest common measure of N and K is Q (> 1). Let $R = N/Q$ and $P = K/Q$. In this case, a partial cyclic symmetry breaking bifurcation occurs. Intuitively, this type of bifurcation occurs due to the fact: $\alpha(K)^R = 1$. The bifurcation diagrams are the same as in Fig. 1 except that the five solutions without the cyclic symmetry in Fig. 1 are replaced by R solutions with the Q-th order cyclic symmetry. The solutions with the Q-th order cyclic symmetry may bifurcate through another cyclic symmetry breaking bifurcation. The effect of the reverse symmetry is the same as in the $\alpha(K)$ case above.

5 Features of MFA procedure

In Sec. 4, local descriptions of the MFA bifurcation processes are shown. In this section, the MFA procedure, which is a series of bifurcations, is discussed.

1. **Non-deterministic feature**
   Figure 2a is a typical example showing a bifurcation diagram of a 5-city TSP, where $V_{1,i}$ $(i = 1, ..., 5)$ of every minimum are plotted against temperature. Figure 2b is the corresponding free energy diagram. When $T > 0.69$, there is a unique minimum $\mathbf{V}^s$ with the 5th order cyclic and reverse symmetries. At $T \approx 0.69$, and 0.67, saddle-node bifurcations occur, and ten minima appear simultaneously. At $T \approx 0.615$, a cyclic symmetry breaking bifurcation occurs, and $\mathbf{V}^s$ bifurcates into five minima without the cyclic symmetry but with the 1st order reverse symmetry. Because of the reverse symmetry, there are only three cascades observed in Fig. 2a. At $T \approx 0.61$, a reverse symmetry breaking bifurcation occurs, and each of the five minima with the 1st order reverse symmetry collides with saddle-points and eventually becomes a saddle-point. After this bifurcation, the annealing solution disappears like in Fig. 1d. At this temperature, there exist two sets of minima, which are generated through saddle-node bifurcations. The free energy levels of those minima are lower than that of the disappearing minima as Fig. 2b shows. In this case, due to the instability of the disappearing bifurcation point, which minimum is found is ambiguous, even though the procedure is deterministic. This implies a non-deterministic property of the deterministic MFA procedure.

2. **Free energy crossing**
   We can observe this phenomenon in Figures 3a and 3b, which are the bifurcation diagram of another 5-city TSP and the corresponding free energy diagram, respectively. At $T \approx 0.61$, the symmetric minimum disappears and the annealing solution changes to one of the minima that appear at $T \approx 0.67$. However, the free energy levels of these annealing minima and the new born minima that appear at $T \approx 0.60$ cross one another and the free energy level of the annealing minima becomes higher than that of the new born minima. After the crossing, the annealing solution turns into a local minimum. In fact, the new born minima correspond to the optimal solution and the annealing minima do not correspond to any of the valid Hamilton passes. In this case, the MFA deterministically results in a failure.

Accordingly, the MFA procedure does not necessarily give a unique minimum solution, even though the procedure is deterministic. And, it does not guarantee the optimal solution, either. Adverse situations have been found to occur more often as the number of cities becomes large. Therefore, the MFA has a non-deterministic property and results in relatively good, i.e., "not-so-bad" solutions, in general. Careful annealing does not necessarily improve these properties.

Let us briefly discuss the convergence. Figure 2c shows the convergence time that corresponds to the bifurcation diagram shown in Fig. 2a. The ordinate indicates the number of rounds until the difference of the MFT solution $\delta \mathbf{V}$ in a round becomes smaller than 10^{-6}. In a round, all the variables are updated exactly once. When a cyclic symmetry breaking bifurcation or a reverse symmetry breaking bifurcation occurs, it takes a long time to converge. However, the latter is much shorter than the former.

6 Algorithm modifications

6.1 Suppressing cyclic symmetry breaking

Cyclic symmetry breaking bifurcations are quite time consuming for convergence, because the free energy has quite a flat surface around the bifurcation point. We can eliminate cyclic symmetry breaking bifurcations by clamping the tour starting city, like: $V_{1,0} = 1, V_{1,n} = 0\ (n = 1, ..., N)$. This means the salesman starts from city 1. Figure 4a is the modified bifurcation diagram for the same 5-city TSP as in Fig. 2. Figure 4b shows the convergence time. Since only reverse symmetry breaking bifurcations occur with this modification, the convergence time becomes much shorter than that in the original MFA shown in Fig. 2c. Although this technique changes the free energy function (3.2) when $T > 0$, it does not worsen the obtained solutions. In fact, it improves them.

In Table 1, we compare the modified MFA with the original MFA. The temperature is decreased as: $\delta T = 10^{-3}$, and the convergence is determined as: $\delta \mathbf{V} = 10^{-6}$. The parameter A is set to be $1.5 \sim 1.6$ in the original MFA, and $1.8 \sim 1.9$ in the modified one. We prepared five testbeds for evaluation; they are 10-city, 20-city, 30-city, 40-city, and 50-city TSPs. Each testbed consists of 100 sets of city allocations that are randomly generated in a unit square. The annealing procedure starts at a fixed temperature for all city allocations; $T_{init} = 1.5$ for the $10 \sim 40$ city testbeds, and $T_{init} = 0.8$ for the 50-city testbed. In each column of the table, the three figures denote the number of valid tours obtained among the 100 sets, the averaged tour length, and the averaged convergence time (divided by 10^4 for displaying convenience), respectively. The tour length and the convergence time are averaged over the cases where valid tours are obtained.

Table 1

	10	20	30	40	50
original	100	96	98	91	88
	3.571	4.695	5.861	6.640	7.313
	3.47	3.20	2.74	2.51	1.92
modified	98	99	96	99	93
	3.561	4.661	5.690	6.548	7.261
	1.27	1.42	1.48	1.57	1.30

The convergence time is much shorter in the modified algorithm. If we employ more rough annealing, i.e., use a bigger δT, this improvement of the convergence time becomes more prominent. Moreover, the solutions of the modified algorithm are better than those of the original one.

6.2 MFT from a saddle point

The disappearance of the annealing solution and saddle-node appearances of the other mimima that can be observed in Figures 2a and 3a are very typical phenomena. The minima generated through saddle-node bifurcations do not disappear, in general. Therefore, if the disappearing point, T_c^d and $\mathbf{V}^d$, is known, the MFA is nothing but a procedure that obtains an MFT solution starting from $\mathbf{V}^d$ at the fixed temperature T_c^d.

Although there is no general way of obtaining T_c^d without the annealing procedure, we can instead obtain the first cyclic symmetry breaking bifurcation temperature T_c^s. When the unique symmetric minimum $\mathbf{V}^s$ disappears through a cyclic symmetry breaking bifurcation as in Fig. 3a, $T_c^d = T_c^s$ and $\mathbf{V}^d = \mathbf{V}^s$. When the minima, whose cyclic symmetry has been broken, disappear through a reverse symmetry breaking bifurcation as in Fig. 2a, T_c^d is a little lower than T_c^s and $\mathbf{V}^d$ is close to $\mathbf{V}^s$. The symmetric solution $\mathbf{V}^s$ can be obtained with the reduced free energy (3.3), which is represented by N_0 variables and converges much faster than the original free energy (3.2). By using the fact that $\mathbf{V}^s$ is stable in the free energy (3.2) for $T > T_c^s$ and unstable for $T < T_c^s$, we can estimate T_c^s through a rough temperature lowering. The stability of the symmetric solution can be found by calculating the minimal eigenvalue in the reduced eigen equation (3.6). Since the disappearing temperature T_c^d is lower than T_c^s, we can obtain T_c^d by conducting an annealing procedure starting from T_c^s. Alternatively, T_c^d can be approximated just as a slightly lower temperature than T_c^s. $\mathbf{V}^d$ can be approximated as the symmetric solution at the approximated T_c^d.

The above-mentioned approximation procedure needs a much smaller computation time than the original MFA procedure. After we can approximate the disappearing point, it is sufficient to obtain the MFT solution starting from the approximated $\mathbf{V}^d$ at the approximated T_c^d without the annealing procedure. Furthermore, we can select the best among many MFT solutions obtained by putting small random terms on the initial condition. This algorithm is faster and can achieve better results than the MFA procedure.

Let us show some experimental results. In the experiment, T_c^d is estimated at $(0.8 \cdot T_c^s)$, and T_c^s is obtained by evaluating the minimal eigenvalue of the free energy curvature. By starting from the neighborhood of the approximated disappearing point, ten MFT solutions are obtained and the best among them is selected. When this algorithm was applied to the above-mentioned 10-city TSPs, 95 tours were obtained and the average tour length was 3.536. As for 20-city TSPs, 90 tours were obtained and the average tour length was 4.574. These results are a little better than that of the original MFA shown in Table 1. If more MFT solutions are obtained,

the results must even improve.

7 Conclusion

In this report, we investigated the MFT bifurcation processes when MFT is applied to TSPs. Due to the cyclic and reverse symmetries of the TSP energy function, some special bifurcations occur. And those bifurcation processes result in the properties of the MFA procedure. The MFA has a non-deterministic property, even though the procedure is deterministic. Moreover, it does not guarantee the optimal solution. The cyclic symmetry breaking bifurcations and the reverse symmetry breaking bifurcations, which are typically observed in the MFA, are quite time consuming for convergence.

In this report, we also proposed a couple of modified algorithms. One is an algorithm that clamps the tour starting city to eliminate the time-consuming cyclic symmetry breaking bifurcations. The other is an annealing-free algorithm, where the MFT solutions are obtained starting from the symmetric saddle point. These algorithms are much faster than the original MFA, while the obtained solutions are better than those of the MFA.

The MFT bifurcation diagrams and the "non-deterministic" and "non-optimal" properties of the MFA procedure are almost equal to those for the Potts spin. This result was briefly mentioned in our previous report.[5]

References

[1] Hopfield, J. J. (1984). *Proceedings of the National Academy of Science, USA*, **81**.

[2] Hopfield, J. J., and Tank, D. W. (1985). *Biological Cybernetics*, **52**.

[3] Peterson, C., and Anderson, J. R. (1987). *Complex Systems*, **1**.

[4] Peterson, C., and Anderson, J. R. (1988). *Complex Systems*, **2**.

[5] Ishii, S. (1995). *IEICE Technical Report*, **NC95-4**.

[6] Van den Bout, D. E., and Miller III, T. K. (1989). *Biological Cybernetics*, **62**.

[7] Wilson, G. W., and Pawley, G. S. (1988). *Biological Cybernetics*, **58**.

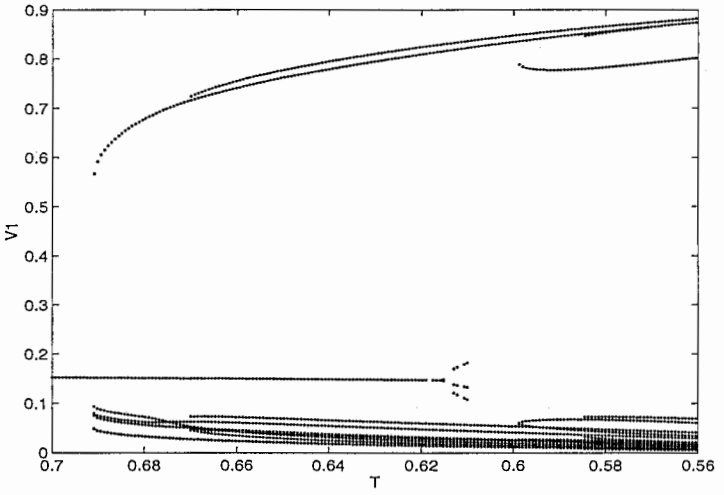

Figure 2a

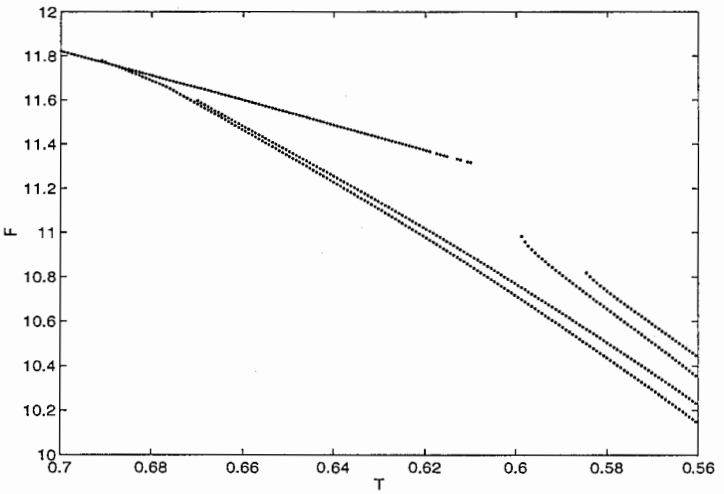

Figure 2b

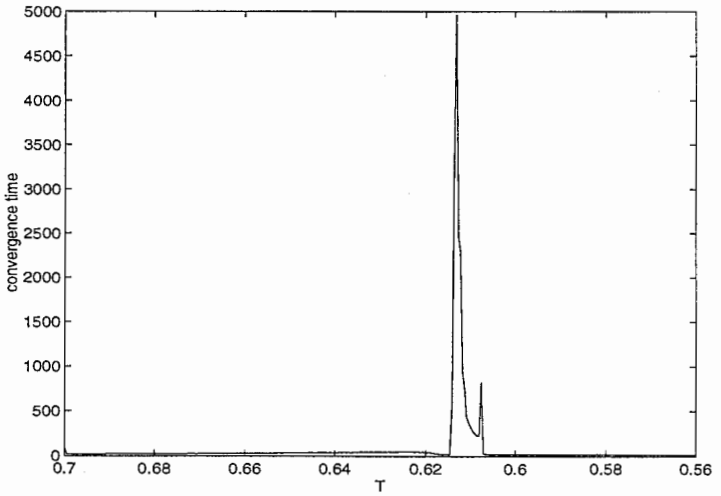

Figure 2c

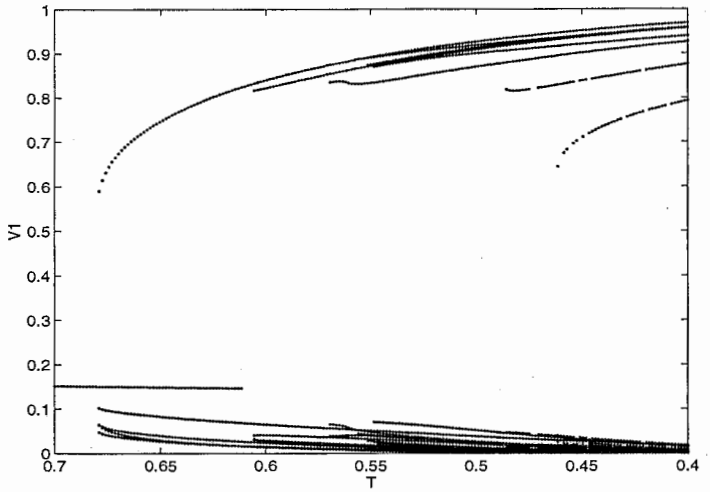

Figure 3a

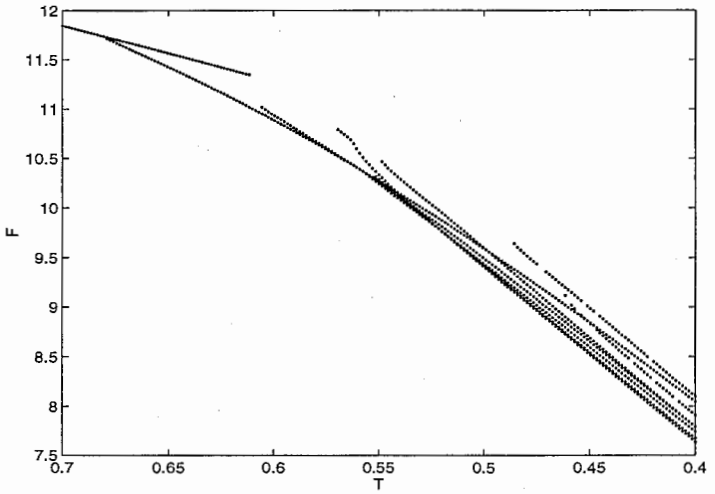

Figure 3b

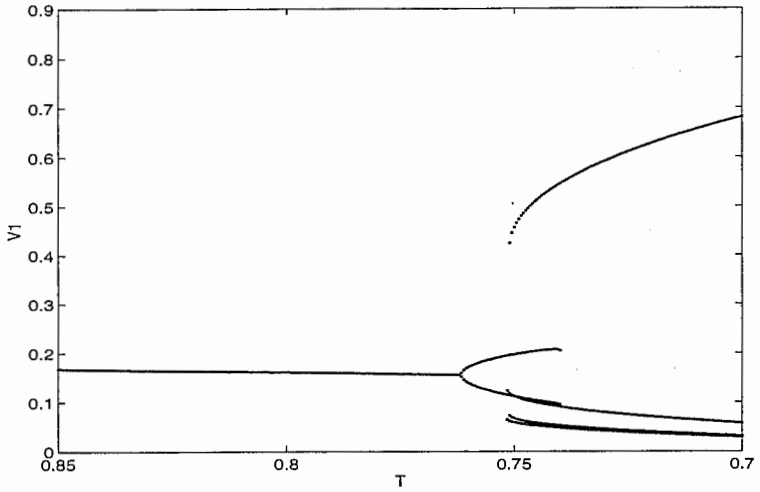

Figure 4a

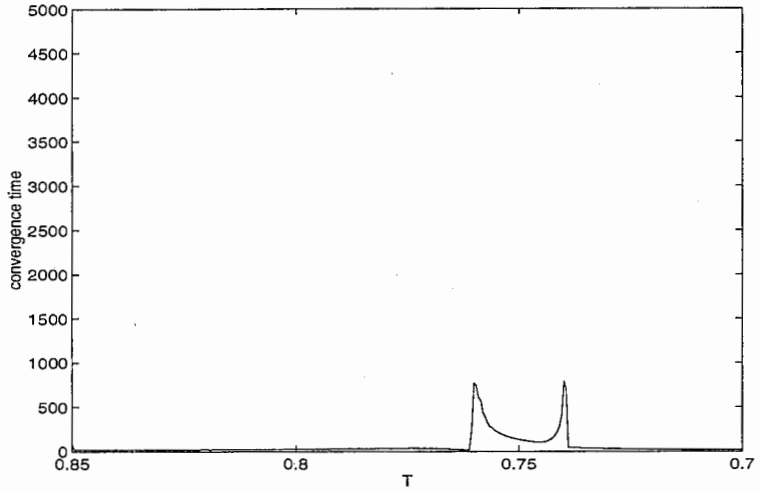

Figure 4b